INFECTION AND IMMUNITY, Sept. 2007, p. 4245–4254 Vol. 75, No. 9
0019-9567/07/$08.00+0 doi:10.1128/IAI.00031-07

Pneumolysin Causes Neuronal Cell Death through Mitochondrial Damage▽

Johann S. Braun,[1,3]*† Olaf Hoffmann,[1]† Miriam Schickhaus,[1] Dorette Freyer,[1] Emilie Dagand,[1] Daniela Bermpohl,[1] Tim J. Mitchell,[4] Ingo Bechmann,[2] and Joerg R. Weber[1,2]

Departments of Neurology[1] and Cell Biology and Neurobiology,[2] Charité Universitaetsmedizin Berlin, Berlin, Germany; Division of Neurology, Department of Internal Medicine, Faculty of Medicine and Health Sciences, United Arab Emirates University, Al Ain, United Arab Emirates[3]; and Division of Infection and Immunity, University of Glasgow, Glasgow, United Kingdom[4]

Received 7 January 2007/Returned for modification 21 February 2007/Accepted 1 June 2007

Bacterial toxins such as pneumolysin are key mediators of cytotoxicity in infections. Pneumolysin is a pore-forming toxin released by *Streptococcus pneumoniae*, the major cause of bacterial meningitis. We found that pneumolysin is the pneumococcal factor that accounts for the cell death pathways induced by live bacteria in primary neurons. The pore-forming activity of pneumolysin is essential for the induction of mitochondrial damage and apoptosis. Pneumolysin colocalized with mitochondrial membranes, altered the mitochondrial membrane potential, and caused the release of apoptosis-inducing factor and cell death. Pneumolysin induced neuronal apoptosis without activating caspase-1, -3, or -8. Wild-type pneumococci also induced apoptosis without activation of caspase-3, whereas pneumolysin-negative pneumococci activated caspase-3 through the release of bacterial hydrogen peroxide. Pneumolysin caused upregulation of X-chromosome-linked inhibitor of apoptosis protein and inhibited staurosporine-induced caspase activation, suggesting the presence of actively suppressive mechanisms on caspases. In conclusion, our results indicate additional functions of pneumolysin as a mitochondrial toxin and as a determinant of caspase-independent apoptosis. Considering this, blocking of pneumolysin may be a promising cytoprotective strategy in pneumococcal meningitis and other infections.

Bacterial toxins are key mediators of cytotoxicity to the host in invasive infections. *Streptococcus pneumoniae* is one of the most common and most aggressive causes of pneumonia and sepsis, and it represents one of the most frequent and most disastrous pathogens in bacterial meningitis. A major exotoxin of *Streptococcus pneumoniae* is pneumolysin (24). Pneumolysin is a multifunctional bacterial cytoplasmic protein of 53 kDa with a wide range of cytotoxic and proinflammatory properties, and it is an important determinant of pneumococcal virulence (28).

Proinflammatory effects of pneumolysin include complement activation, enhanced activation of neutrophils (10), and increased production of proinflammatory mediators such as tumor necrosis factor alpha, interleukin-1β, and nitric oxide (5, 28). Pneumolysin activates the innate immune system through Toll-like receptor 4 (TLR4) (34). Upon intrathecal application, it triggers an acute inflammatory response equivalent to the effects of live bacteria (15). However, pneumolysin is not required in order to induce an immune response to pneumococci (2, 15, 39).

Pneumolysin shares cytotoxic properties with a large family of highly homologous thiol-activated cytolysins (25). Other members of this group are streptolysin (*Streptococcus pyogenes*), perfringolysin (*Clostridium perfringens*), and listeriolysin (*Listeria monocytogenes*). Pneumolysin binds to the cholesterol of eucaryotic cell membranes and induces pore formation (3, 16). In the respiratory tract, destruction of tissue barriers leads to enhanced pulmonary inflammation and injury (31) as well as to septic dissemination of *S. pneumoniae* (1, 30).

In pneumococcal meningitis, pneumolysin causes the death of cochlear cells and subsequent hearing loss (12, 40). Independently of the inflammatory response, pneumolysin also mediates neuronal loss in the dentate gyrus, where it is colocalized with neurons undergoing apoptosis (4). The specific events involved in the direct toxicity of pneumolysin toward neurons are not known. Live pneumococci cause neuronal cell death by inducing rapid increases in the levels of intracellular reactive oxygen species (ROS) and calcium (Ca^{2+}), followed by early mitochondrial damage and release of the mitochondrial apoptosis-inducing factor (AIF) (7). In the present study, we hypothesized a role for pneumolysin as a mediator of these effects of live bacteria.

MATERIALS AND METHODS

Materials. Standard chemicals, acridine orange, ethidium bromide, staurosporine, dimethyl sulfoxide, and components of the lactate dehydrogenase assay and of the bacterial growth medium were obtained from Sigma (Deisenhofen, Germany). Cell culture medium and supplements were from Gibco, United Kingdom. Fluo-4, tetramethyl rhodamine ethyl ester (TMRE), and 123-rhodamine were purchased from Molecular Probes, Eugene, OR. Components of the caspase activity assays and *N*-benzyloxycarbonyl-Val-Ala-Asp fluoromethylketone (z-VAD-fmk) were from Calbiochem, San Diego, CA. Pneumolysin was purified as previously described (5). Hemolytic activity was verified qualitatively by dropping eluted pneumolysin fractions onto sheep blood agar plates. We also used the Trp-433→Phe (W433F) pneumolysin point mutant, which has substantially (1,000-fold) decreased pore-forming activity (24).

Neuronal cell culture. Primary rat cortical neurons were obtained from fetal rats on embryonic day 18. Cultures were prepared as described previously (21). Plates were coated with poly-L-lysine and collagen. Briefly, the cortex or hippocampus was dissected, incubated in trypsin-EDTA (Biochrom, Berlin, Germany), dissociated with a Pasteur pipette, and plated in starter medium (serum-free neurobasal medium supplemented with B27, 0.5 mM glutamine, 100 U/ml penicillin/streptomycin, and 25 μM glutamate), and cells were counted and plated in 48- or 96-well plates at a density of 150,000/cm^2. The status of cultures

* Corresponding author. Mailing address: United Arab Emirates University, Faculty of Medicine and Health Sciences, Department of Internal Medicine, Division of Neurology, P.O. Box 17666, Al Ain, United Arab Emirates. Phone: 971 3 7137 419. Fax: 971 3 7672 995. E-mail: johannb@uaeu.ac.ae.

† J.S.B. and O.H. contributed equally to this work.

▽ Published ahead of print on 11 June 2007.

was assessed by light microscopy, immunohistochemistry, and a trypan blue exclusion test as described previously (21). On day 8, neurons were exposed to pneumolysin at various concentrations (20 to 500 ng/ml), depending on the experiment and the readout.

Bacterial cell culture. D39 capsular type 2 *Streptococcus pneumoniae* (Rockefeller University, New York, NY) and its isogenic pneumolysin-deficient Δ*plnA* (1) and Δ*plnA* Δ*spxB* (4) mutants were grown in casein-plus-yeast (C+Y) medium to an optical density at 620 nm of 0.4 to 0.6, pelleted, and resuspended in sterile phosphate-buffered saline (PBS). The bacterial inoculum was prepared by adjusting the bacterial concentration to various CFU per milliliter using a photometer. Bacteria were plated onto blood agar plates to confirm quantity and viability.

Cytotoxicity assays and differentiation between apoptosis and necrosis. Intracellular reduction of the tetrazolium salt 3-(4,5-dimethylthiazol-2-yl)2,5-diphenyl tetrazolium bromide (MTT) to a purple formazan was used to determine neuronal cell viability (26). Following exposure of neurons to pneumolysin, the MTT labeling agent was added (final concentration, 0.5 mg/ml) and the absorbance of the formazan product was measured at 550 nm. DNA laddering was performed according to the protocol described previously (21). The in situ cell death TUNEL (terminal deoxynucleotidyltransferase-mediated dUTP-biotin nick end labeling) detection kit (Boehringer, Mannheim, Germany) was used as described by the manufacturer. Ethidium bromide and acridine orange (Sigma) are fluorescent intercalating DNA dyes. Acridine orange stains all nuclei green, whereas ethidium bromide stains nuclei red but is excluded by cells with an intact cell membrane. Double staining with ethidium bromide and acridine orange (both used at a concentration of 2 μg/ml) allows differentiation of live, apoptotic, and necrotic cells on the basis of nuclear size and color (7).

Fluorometric analysis of caspase activities. Following incubation with pneumolysin for different times, neurons were scraped, centrifuged at 2,000 rpm, and lysed in 50 mM HEPES–1 mM dithiothreitol–0.1 mM EDTA–0.1% 3-[(3-cholamidopropyl)-dimethylammonio]-1-propanesulfonate (CHAPS) (pH 7.4) for 5 min on ice. Lysates were centrifuged at 15,000 rpm, and supernatants (20 μl) were added to 80 μl of reaction buffer (100 mM NaCl, 50 mM HEPES, 10 mM dithiothreitol, 1 mM EDTA, 10% glycerol, 0.1% CHAPS [pH 7.4]) containing 75 μM of a specific fluorogenic caspase substrate (Calbiochem, San Diego, CA). After incubation at 37°C for 60 min, fluorescence was measured by a microplate reader (CytoFluor II; PerSeptive Biosystems, Framingham, MA). Standard AMC (7-amino-4-methyl coumarin) and AFC (7-amino-4-trifluoromethyl coumarin) solutions were used for calculating caspase activity.

Immunocytochemistry. Primary rat neurons were incubated with pneumolysin, fixed (with 4% paraformaldehyde), and permeabilized (with 0.1% Triton X-100). These neurons were processed for immunocytochemistry, with an anti-AIF antibody (Santa Cruz, Santa Cruz, CA) diluted 1:500 in PBS–1% bovine serum albumin, or for TUNEL staining (Boehringer). A fluorescent Cy3 antibody (Jackson ImmunoResearch, West Grove, PA) was used to visualize the binding sites of the primary antibody.

Assessment of mitochondrial membrane potential. TMRE (Molecular Probes) was used to assess the integrity of the mitochondrial membrane potential as described previously (18). Following incubation with pneumolysin, TMRE was added (at 300 nM for 30 min) to neurons, and its mitochondrial uptake was assessed by fluorescence microscopy and in the CytoFluor II multiwell fluorescence plate reader.

Calcium assay. Changes in intracellular calcium concentrations were monitored with Fluo-4. Following exposure to pneumolysin, neurons were incubated with Fluo-4 (at 10 μM for 30 min) and rinsed with PBS, and intracellular calcium concentrations were determined by fluorescence. Fluorescence was determined with a multiwell fluorescence plate reader (CytoFluor II).

Assay for ROS. Changes in intracellular ROS concentrations were monitored with the ROS-specific dye dihydrorhodamine 123 (DHR 123) using a multiwell fluorescence plate reader (Cytofluor II). DHR 123 fluoresces when oxidized to rhodamine 123. Neurons were preincubated with 10 μM DHR 123 for 1 h, followed by exposure to pneumolysin.

Western blotting. Primary rat neurons were incubated with pneumolysin (at 500 ng/ml for 6 h). Whole neurons were pelleted by centrifugation, and pellets were lysed on ice in radioimmunoprecipitation assay buffer (50 mM Tris, 150 mM NaCl, 1% Triton X-100, 0.1% sodium dodecyl sulfate, and 1% sodium deoxycholate) with 10 mg/ml protease inhibitor mixture (Boehringer, Mannheim, Germany). Subcellular fractionation by differential centrifugation, homogenization, and digitonin treatment was performed according to the protocol of Bronfman and coworkers (9). The protein extracts were separated by sodium dodecyl sulfate-polyacrylamide gel electrophoresis and transferred to a polyvinylidene membrane. Blots were blocked and incubated with an anti-caspase-3 primary antibody (1:1,000; New England Biolabs, Frankfurt, Germany) or an anti-AIF antibody (1:300; Santa Cruz, Santa Cruz, CA) overnight at 4°C. Blots were rinsed, incubated with a horseradish peroxidase-conjugated secondary antibody, and developed using the ECL kit (both from Amersham, Little Chalfont, Buckinghamshire, England).

PFGE and internucleosomal DNA fragmentation. Large-scale DNA fragments were detected by pulsed-field gel electrophoresis (PFGE), which was performed as described elsewhere (33). Briefly, cell pellets were embedded in agarose, and agarose plugs were incubated in digestion buffer (0.5 M EDTA, 1% laurylsarcosine, 1 mg/dl proteinase K) for 36 h at 50°C. Thereafter, agarose pellets were washed in 0.5× Tris-boric acid-EDTA buffer, loaded onto a gel, and separated by alternating-current electrophoresis in a Bio-Rad CHEF-DR II hexagonal chamber (Bio-Rad Laboratories) (1% agarose; 0.5× Tris-boric acid-EDTA; 190 V; 24 h; pulse wave, 60 s; 120° angle). Molecular weight standards (λ ladder PFG marker and low-range PFG marker) were purchased from New England Biolabs.

To investigate internucleosomal DNA fragmentation, neurons were exposed to pneumolysin or staurosporine, and agarose gel electrophoresis of DNA was performed as described previously (23). DNA was isolated from neurons (10^6) by using a genomic DNA isolation kit (Invitrogen Corp.) according to the manufacturer's instructions.

Electron and immune electron microscopy. Primary rat neurons were exposed to pneumolysin and its pore formation-deficient mutant for 3 and 6 h. Thereafter, neurons were rinsed twice with PBS and fixed overnight at 4°C with 3% glutaraldehyde and 3% paraformaldehyde in ice-cold PBS. Neurons were postfixed in a solution of osmium tetroxide (0.7% in PBS) and 0.2 M sucrose. Neurons were dehydrated; incubated twice in pure hydroxypropylmetacrylate (HPMA; Fluka, Neu-Ulm, Germany), twice in a mixture of 50% HPMA and 50% Epon 812 with accelerators (Fluka), and twice in 100% Epon with accelerators; and finally embedded in Epon. Ultrathin sections were cut with a Reichert Ultracut S ultramicrotome (Leica, Vienna, Austria) with a diamond knife and were mounted on grids (Plano, Marburg, Germany) coated with Formvar film (Fluka). These sections were stained with a Reichert UltraStainer (Leica) using uranyl acetate and lead citrate and were examined in an EM900 electron microscope (Zeiss, Germany).

For immune electron microscopy, neurons were exposed to pneumolysin (at 200 ng/ml for 5 and 10 h) and fixed overnight at 4°C with 0.2% glutaraldehyde and 3% paraformaldehyde in ice-cold PBS. Thereafter, cells were rinsed extensively in PBS and immunocytochemistry was performed using a polyclonal antibody against pneumolysin diluted 1:200 in PBS–1% bovine serum albumin (Novocastra, Newcastle upon Tyne, United Kingdom). A biotinylated secondary antibody, the ABC system, and diaminobenzidine (Vector, Burlingame, CA) were used to detect the binding sites of the primary antibody.

TLR4 real-time PCR. To quantify TLR4 receptor mRNA expression, total RNA was isolated from ~10^6 cells by applying standard methods using TRIzol reagent (Life Technologies). DNA was removed by DNase incubation (Promega, Mannheim, Germany), followed by phenol-chloroform extraction and ethanol precipitation. RNA was quantified by determining optical density. Reverse transcription of 2 μg extracted RNA was performed with random hexamer primers (Roche Applied Science, Mannheim, Germany) and Moloney murine leukemia virus reverse transcriptase (Promega) according to the manufacturer's instructions. Real-time PCR was performed using FastStart DNA SYBR green I and a LightCycler (Roche). PCR conditions were as follows: 10 min at 95°C, followed by 45 cycles at 95°C for 15 s, 64°C for 10 s, and 72°C for 15 s (amplification product data acquisition at 81°C). The mean cycle threshold value was used for analysis. The TLR4 expression of each sample was normalized on the basis of its β-actin and glyceraldehyde-3-phosphate dehydrogenase (GAPDH) mRNA content. The following sequence-specific primers were used: TLR4 forward, 5′-AG CAGGTCGAATTGTATCGC-3′; TLR4 reverse, 5′-TGTGAGGTCGTTGAG GTTAG-3′; beta-actin forward, 5′-ACCCACACTGTGCCCATCTA-3′; beta-actin reverse, 5′-GCCACAGGATTCCATACCCA-3′; GAPDH forward, 5′-AG ATTGTCAGCAATGCATCCTGC-3′; GAPDH reverse, 5′-CCTTCTTGATGT CATCATACTTGG-3′.

TLR4 in situ hybridization. The digoxigenin (DIG)-labeled sense and antisense RNA probes of rat TLR4 were prepared as follows. The 299-bp fragment of the rat TLR4 cDNA was amplified using the primers mentioned above and subcloned into the pGEM-T vector (Promega). The plasmid was linearized and taken as a template for generation of DIG-labeled RNA probes using SP6 or T7 RNA polymerase according to the manufacturer's protocol (Roche, United States). These probes were used for in situ hybridization on primary rat neurons or microglia according to the method of Breitschopf and coworkers (8). Primary brain cells were grown on glass slides for 8 days, then fixed with paraformaldehyde, and finally pretreated with proteinase K. Hybridization was performed overnight at 63°C in a moist chamber. After rinsing three times and blocking (with 10% fetal calf serum in PBS), the binding sites were visualized using a

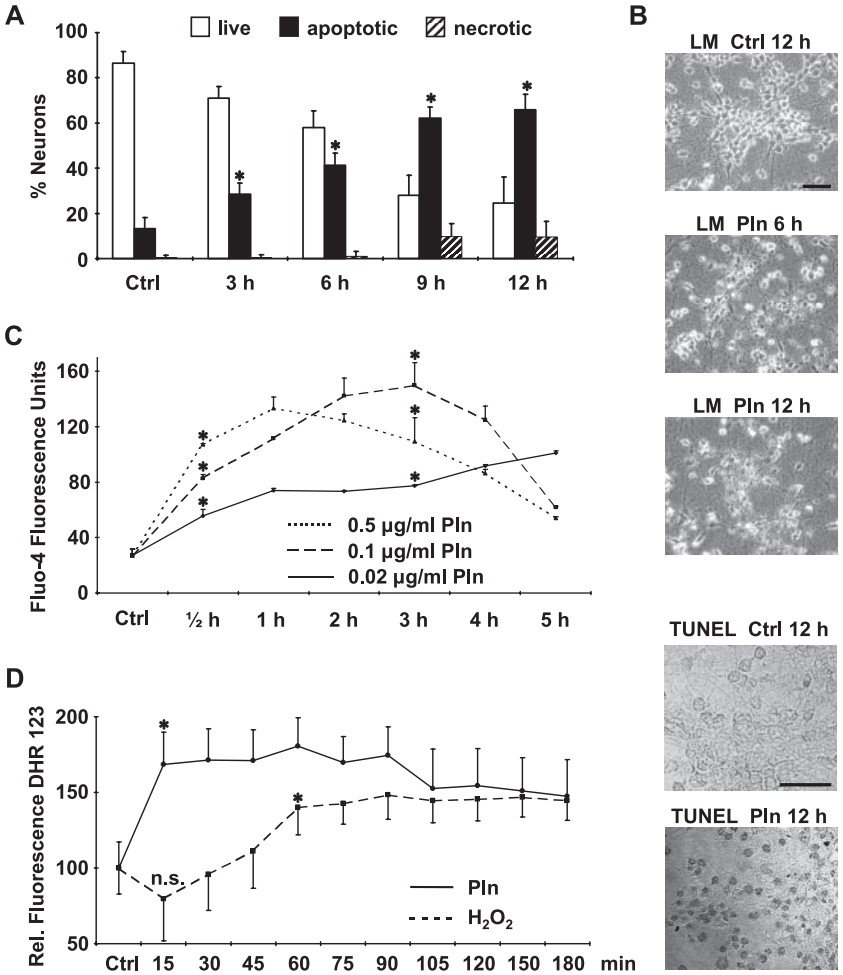

FIG. 1. Pneumolysin induces increases in intraneuronal calcium and ROS levels and causes cell death. Primary rat cortical neurons were either incubated with pneumolysin (500 ng/ml) or left untreated as a control (Ctrl). (A) Apoptosis and necrosis were differentiated and quantified with the nuclear dyes acridine orange and ethidium bromide. (B) Evidence of apoptosis by light microscopy (LM) and TUNEL of neurons treated with pneumolysin (Pln) (500 ng/ml). Bars, 30 μm. (C and D) Intraneuronal levels of Ca^{2+} (C) and ROS (D) were visualized by the fluorescence of the dyes Fluo-4 (10 μM) and DHR 123 (10 μM), respectively. Results shown (means + standard deviations) are representative of three independent experiments performed in triplicate, *, $P < 0.05$ for comparison with the control by Student's *t* test; n.s., no significant difference from the control.

fluorescein-conjugated anti-DIG antibody (1:1,000) (Boehringer, Mannheim, Germany).

RESULTS

Pneumolysin causes apoptosis in primary neurons. The kinetics of pneumolysin-induced neurotoxicity were determined and quantified by the acridine orange-ethidium bromide assay (Fig. 1A), the MTT assay, and light microscopy (Fig. 1B). Pneumolysin was a potent inducer of primary neuronal cell death. Cellular and nuclear shrinkage and condensation were detectable as early as 3 h after the start of incubation with pneumolysin and increased time-dependently (Fig. 1A and B). Further markers of apoptotic cell death were the loss of neuronal processes and the induction of DNA double-strand breaks as evidenced by the TUNEL reaction (Fig. 1B).

Pneumolysin increases intraneuronal calcium (Ca^{2+}) and ROS levels. Live pneumococci are known to induce rapid increases in intracellular ROS and Ca^{2+} levels. We therefore assessed whether pneumolysin is also able to increase ROS and Ca^{2+} levels.

Intracellular Ca^{2+} levels were determined by measuring Fluo-4 fluorescence. A marked increase in the cytosolic Ca^{2+} level was detected as early as 30 min after the addition of pneumolysin (Fig. 1C). The kinetics of intracellular Ca^{2+} increase were dose dependent. Peak fluorescence was reached at 1 h with 0.5 μg/ml Pln and at 3 h with 0.1 μg/ml Pln, while the Ca^{2+} level was still increasing at 5 h with 0.02 μg/ml Pln (Fig. 1C).

Intracellular ROS were detected using DHR 123. Uncharged nonfluorescent DHR 123 is oxidized intracellularly to the cationic fluorescent rhodamine 123 derivative in the presence of ROS (20). Neurons were preloaded with DHR 123, followed by incubation with pneumolysin or H_2O_2 as a positive control. Both H_2O_2 and pneumolysin increased the intensity of DHR 123 fluorescence (Fig. 1D). Therefore, increases in intracellular ROS and Ca^{2+} levels precede pneumolysin-induced neuronal apoptosis.

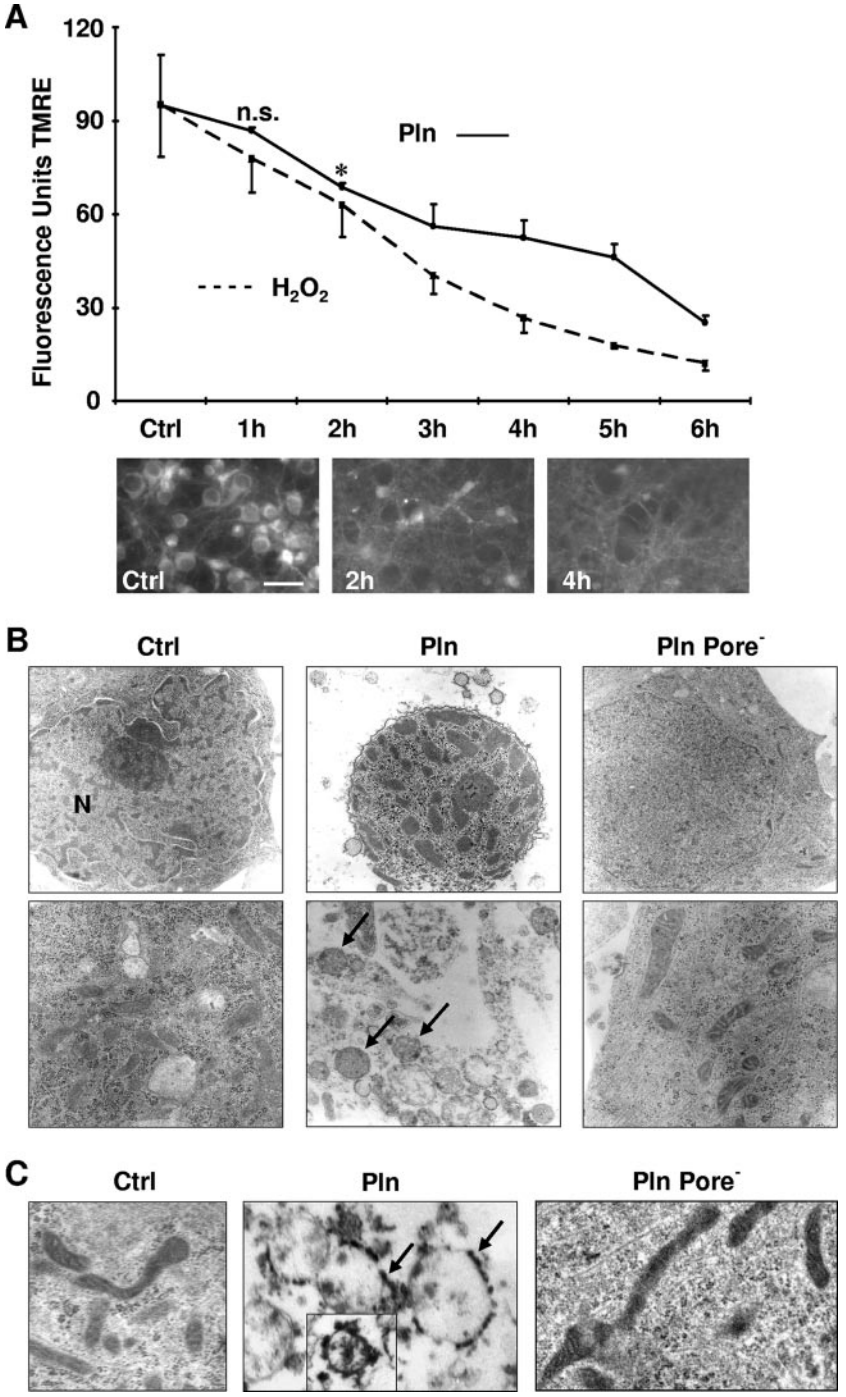

FIG. 2. Pneumolysin damages neuronal mitochondria. (A) Primary rat neurons were incubated with pneumolysin (Pln) (200 ng/ml). Mitochondrial membrane potential integrity was assessed by measuring the uptake of the TMRE dye ($n = 3$) (means + standard deviations). *, $P < 0.05$ for comparison with the control (Ctrl) by Student's t test; n.s., no significant difference from the control. Bar, 20 μm. (B) Neurons were incubated with Pln (500 ng/ml, 6 h), and ultrastructure was monitored by transmission electron microscopy. Control neurons showed intact ultrastructure of the nucleus and mitochondria. Pln caused nuclear shrinkage, chromatin condensation, and massive swelling of cell organelles (arrows). In contrast, in neurons exposed to the Pln mutant defective in pore formation ($Pore^-$), nuclear shrinkage, chromatin condensation, and mitochondrial swelling were markedly impaired. N, nucleus. Magnifications, ×4,000 (top) and ×12,000 (bottom). (C) Following incubation with Pln (200 ng/ml, 5 h), immune electron cytochemistry was performed by applying a Pln-specific antibody. Binding sites of the antibody were visualized with the diaminobenzidine reaction (arrows). Inset shows results at a late time after exposure to Pln (200 ng/ml, 10 h). The Pln mutant defective in pore formation did not bind to mitochondrial membranes. Magnification, ×24,000.

Pneumolysin binds to neuronal mitochondria and damages the mitochondrial membrane potential and ultrastructure. Next, we asked whether pneumolysin is able to trigger mitochondrial damage, and we used the mitochondrion-selective dye TMRE to investigate. The uptake of TMRE depends on an intact mitochondrial membrane potential (22). Control neurons all stained positive with TMRE in a pronounced perinuclear pattern (Fig. 2A). Following exposure to pneumolysin, the mitochondrial TMRE level decreased rapidly (Fig. 2A). In addition, we also observed a marked reduction in the mitochondrial metabolism of MTT (26) as early as 3 h after exposure (data not shown). The loss of mitochondrial membrane potential preceded all morphological signs of apoptosis, e.g., nuclear condensation and shrinkage.

To determine if the loss of mitochondrial membrane potential was associated with ultrastructural changes of mitochondria, we performed electron microscopy at different time points. Exposure of neurons to pneumolysin caused a massive swelling of mitochondria (Fig. 2B). Pneumolysin is known to bind to cholesterol in cell membranes. To test the hypothesis that pneumolysin might also bind to mitochondrial membranes, we used immune electron microscopy on primary neurons after 5 and 10 h of incubation with pneumolysin. Pneumolysin was detected on the membranes of swollen mitochondria by using an anti-pneumolysin antibody (Fig. 2C). Control neurons that were either left untreated (Fig. 2C) or treated with staurosporine (data not shown) did not show binding of the anti-pneumolysin antibody to the mitochondria. In our previous studies, we have shown that the pore-forming activity of pneumolysin is required for its proapoptotic function (4). A pneumolysin point mutant (W433F) with defective (only 0.1%) cytolytic activity failed to induce apoptosis. Therefore, we exposed neurons to W433F mutant pneumolysin and studied its mitochondriotoxic properties. The deficiency in pore formation abolished both mitochondrial swelling and nuclear shrinkage (Fig. 2B) as well as the binding of pneumolysin to mitochondria (Fig. 2C). Thus, the lost proapoptotic potential of W433F mutant pneumolysin most probably is due to its reduced mitochondrial toxicity.

Pneumolysin induces the release of mitochondrial AIF and large-scale DNA fragmentation. Loss of mitochondrial integrity is associated with the release of proapoptotic factors into the cytosol, including AIF, which induces caspase-independent apoptosis (37). Applying immunocytochemistry, we found a decreased mitochondrial localization of AIF within 1.5 h following incubation of neurons with wild-type pneumolysin (Fig. 3A). Mutant pneumolysin defective in pore formation failed to release AIF from mitochondria (Fig. 3A). During pneumolysin-induced neuronal death, AIF decreases in mitochondria, appears in the cytosol, and translocates to the nuclei, as shown by immunoblotting of AIF in mitochondrial and cytosolic neuronal cell fractions (Fig. 3B) and by immunocytochemical double staining of AIF and nuclei (Fig. 3C).

AIF functions as an endonuclease, causing large-scale DNA fragmentation with approximately 50-kb fragments. Both large-scale DNA fragmentation and DNA laddering are markers of apoptosis. There are two pathways leading to apoptosis: one involves caspases and causes oligonucleosomal DNA fragmentation (DNA laddering), while the other is caspase independent, involves AIF, and leads to large-scale DNA fragmentation (38). Since large-scale DNA fragmentation is a signature event in AIF-mediated (caspase-independent) cell death, we tested if pneumolysin-induced release of mitochondrial AIF triggers large-scale DNA fragmentation. Primary rat neurons were either left untreated or incubated with pneumolysin. Staurosporine was used as a positive control. Both staurosporine and pneumolysin induced massive apoptosis of neurons. However, PFGE detected large-scale DNA fragmentation only in neurons exposed to pneumolysin, not in neurons exposed to staurosporine or in control neurons (Fig. 3D).

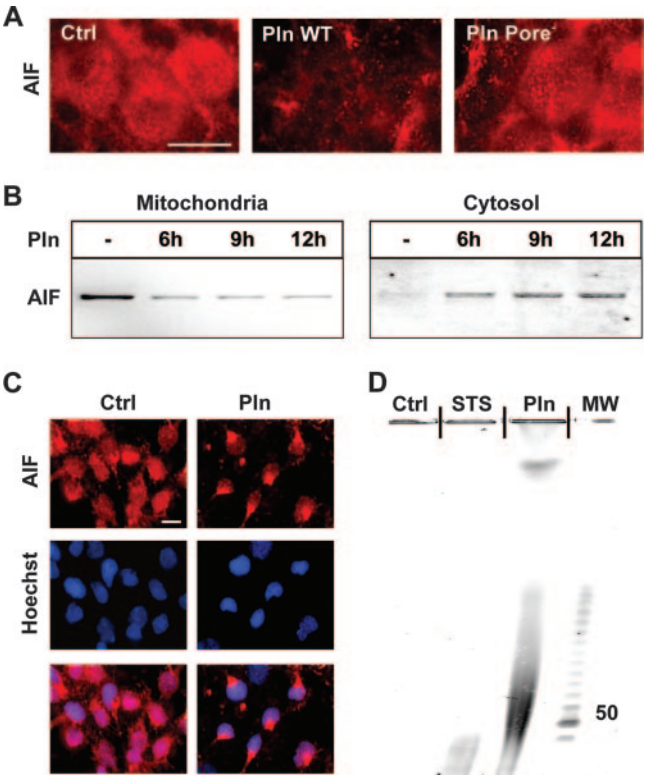

FIG. 3. Pneumolysin (200 ng/ml) induces the release of mitochondrial AIF. (A) Immunocytochemistry of neurons using an anti-AIF antibody. AIF was released from mitochondria following incubation of neurons with pneumolysin (Pln) (200 ng/ml, 9 h) but not with equal concentrations of its mutant deficient in pore formation ($Pore^-$). Ctrl, control. Bar, 10 μm. (B) Western blots of mitochondrial and cytosolic fractions show release of AIF from mitochondria into the cytosol. (C) AIF immunocytochemistry and Hoechst nuclear staining show translocation of AIF to the nucleus. Bar, 10 μm. (D) PFGE of genomic DNA prepared from neurons exposed to Pln (500 ng/ml, 12 h) detected large-scale DNA fragmentation. STS, staurosporine; MW, molecular weight (in thousands).

Pneumolysin fails to induce caspases. Using immunoblotting and caspase activity assays, we evaluated whether pneumolysin activates caspases. Incubation of primary neurons with staurosporine (as a positive control) led to the activation of caspases (Fig. 4A and C) (data not shown for caspases 2, 5, 6, and 9) and caused typical nuclear condensation and fragmentation. In contrast, despite its potent death-inducing activity, pneumolysin failed to activate caspases in primary neurons (Fig. 4A and C). Furthermore, incubation of neurons with pneumolysin in the presence of the broad-spectrum caspase inhibitor z-VAD-fmk did not prevent cell death, whereas staurosporine-induced neuronal

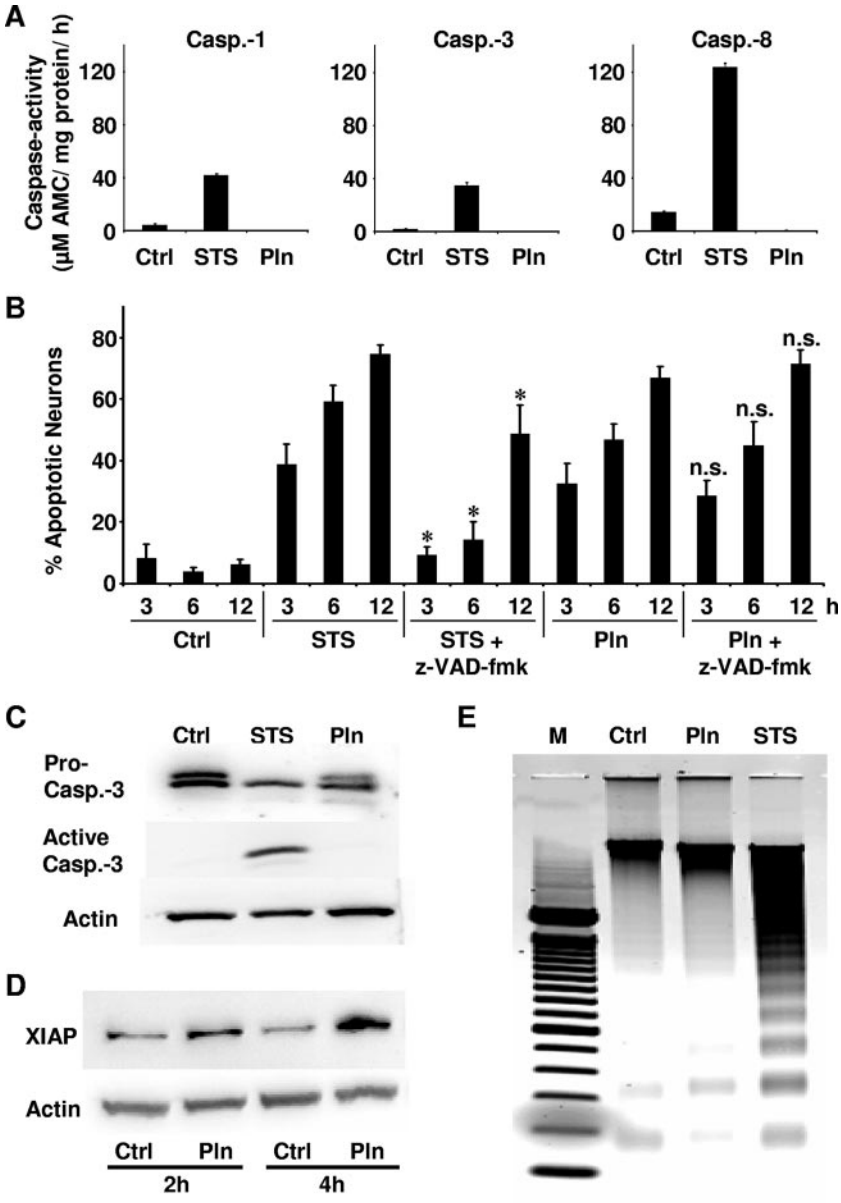

FIG. 4. Pneumolysin induces apoptosis in neurons without activation of caspases. Primary rat neurons were induced to undergo apoptosis by incubation with pneumolysin or staurosporine. (A) Incubation of neurons with staurosporine (STS; 0.1 μM, 5 h) induced caspase (Casp.) activation. Neuronal caspases were not activated following exposure to pneumolysin (Pln; 500 ng/ml, 6 h). Results of representative caspase activity assays for caspase-1, -3, and -8 are shown. Similar results were obtained by measurement of other caspases (data not shown). Each error bar indicates the standard deviation for one of three experiments performed in triplicate. Ctrl, control. (B) Apoptotic neurons quantified by the acridine orange-ethidium bromide assay after exposure to STS (0.1 μM) or Pln (500 ng/ml) with or without z-VAD-fmk (100 μM). *, $P < 0.05$ for comparison with STS by Student's t test; n.s., no significant difference from result for Pln alone. (C) Immunoblotting detected active caspase-3 in cells exposed to STS (0.1 μM, 5 h) but not in cells exposed to Pln (500 ng/ml, 6 h). (D) Western blotting of XIAP was performed with untreated control neurons and with neurons exposed to Pln (200 ng/ml). Actin was used as a loading control. (E) Regular agarose gel electrophoresis. Typical DNA laddering was detected for neurons exposed to STS (0.1 μM, 5 h) but not for those exposed to Pln (500 ng/ml, 6 h).

apoptosis was prevented by z-VAD-fmk (Fig. 4B). Western blotting detected active caspase-3 in staurosporine- but not in pneumolysin-incubated neurons (Fig. 4C). Pneumolysin was actually able to block staurosporine-induced caspase activation. Upon incubation of neurons for 4 h with staurosporine and/or pneumolysin, caspase-3 activities were as follows (by the caspase-3 activity assay): 22.0 ± 3.8 μM with staurosporine, 7.5 ± 1.3 μM with pneumolysin, 12.5 ± 1.2 μM with staurosporine plus pneumolysin, and 11 ± 1 μM for the control.

As a possible mechanism of caspase inhibition by pneumolysin, we found a time-dependent upregulation of the potent caspase-inhibitor XIAP (X-chromosome-linked inhibitor of apoptosis protein) in primary neurons exposed to pneumolysin (Fig. 4D).

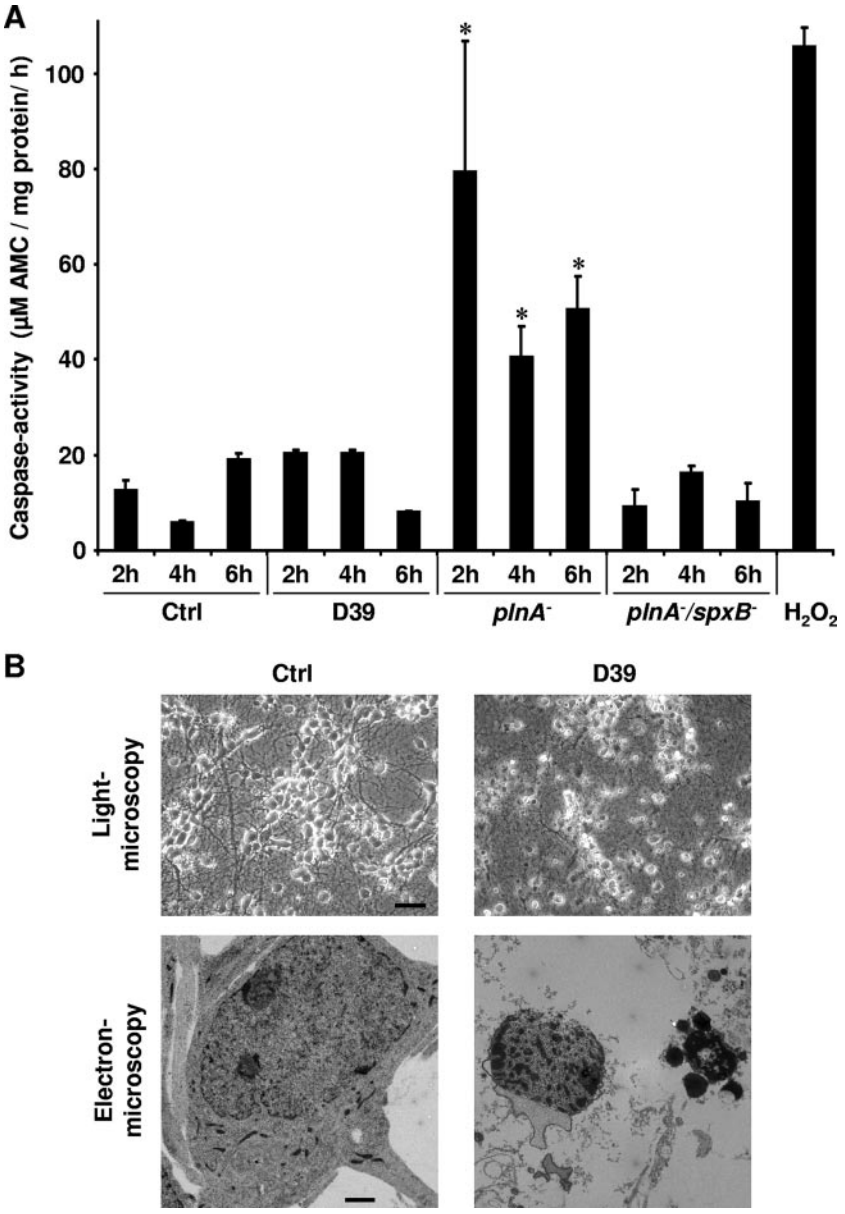

FIG. 5. (A) The pneumolysin-deficient Δ*plnA* mutant but not wild-type *S. pneumoniae* D39 was able to induce caspase-3 activation. Primary rat neurons were incubated with either D39, the Δ*plnA* mutant, or the Δ*plnA* Δ*spxB* double mutant at 10^7 CFU/ml, or with medium alone, for the indicated time points, and caspase-3 levels were determined using the fluorogenic caspase activity assay. Each error bar indicates the standard deviation for one of three experiments performed in triplicate. *, $P < 0.05$ for comparison with the control (Ctrl) or D39 by Student's *t* test. (B) D39 (10^7 CFU/ml, 6 h) potently induced apoptotic morphology, e.g., shrinkage of cells and nuclei, blebbing of nuclear membranes, condensation and fragmentation of nuclei (light microscopy bar, 30 μm; electron microscopy bar, 1 μm) but without activation of caspase-3.

Oligonucleosomal DNA laddering (a typical feature of caspase-mediated cell death) was observed only for primary neurons exposed to staurosporine, not for neurons exposed to pneumolysin or for untreated neurons (Fig. 4E).

Pneumolysin-negative *S. pneumoniae* activates neuronal caspase-3. Neuronal apoptosis induced by live *S. pneumoniae* is independent of caspase activation (7). We therefore tested the hypothesis that the absence of caspase activation in pneumococcus-induced neuronal apoptosis is due to the presence of pneumolysin. Neurons were incubated with either live wild-type bacteria (*S. pneumoniae* serotype 2), the isogenic pneumolysin-negative Δ*plnA* mutant, or the Δ*plnA* Δ*spxB* double mutant deficient in pneumolysin and H_2O_2 production. Caspase-3 activation was investigated at several time points by using the caspase activity assay (Fig. 5A). Wild-type pneumococci did not induce caspase activation above the level of control neurons, although they potently induced apoptotic morphology in light and electron microscopy, e.g., shrinkage of cells and nuclei, blebbing of nuclear membranes, and condensation and fragmentation of

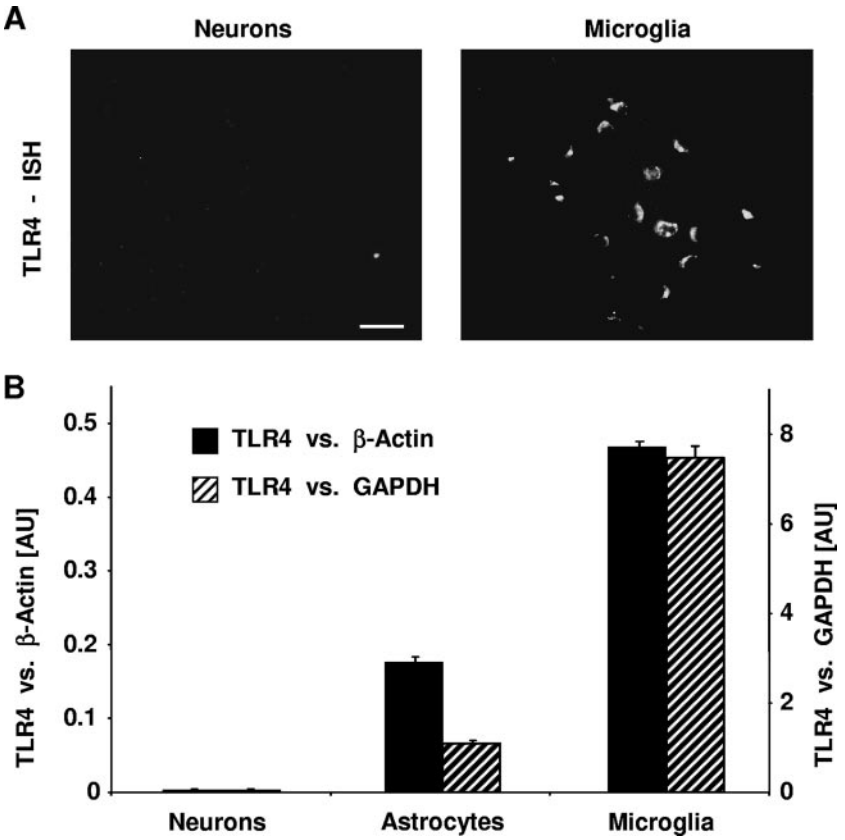

FIG. 6. Pneumolysin-induced apoptosis in primary rat neurons does not require TLR4. (A) In situ hybridization (ISH) of TLR4 on primary rat neurons and primary rat microglia. Binding sites of rat TLR4 antisense RNA probes are visualized with a fluorescent antibody. Bar, 20 μm. (B) Quantitative real-time PCR using β-actin (solid bars) or GAPDH (hatched bars) as an internal standard reveals the highest levels of TLR4 mRNA in microglia and the virtual absence of TLR4 mRNA in neurons. However, both cell types undergo apoptosis by pneumolysin with similar kinetics (data not shown). AU, arbitrary units.

nuclei (Fig. 5B). In contrast, the pneumolysin-negative mutant consistently induced caspase activation at various time points (Fig. 5A). This is not due to different kinetics of caspase activation, since wild-type pneumococci also failed to induce caspase activation at other time points, e.g., after 30, 60, or 90 min of incubation (data not shown). We hypothesized that caspase activation by pneumolysin-deficient pneumococci could be mediated by H_2O_2, another major exotoxin of *S. pneumoniae*. Using the Δ*plnA* Δ*spxB* double mutant, which is defective both in pneumolysin and in H_2O_2, we did not observe caspase activation (Fig. 5A). These findings indicate that in wild-type pneumococci, the caspase-inactivating effects of pneumolysin counteract caspase activation by H_2O_2, leading to the induction of caspase-independent apoptosis.

Pneumolysin-induced apoptosis in neurons does not require TLR4. In the RAW 264.7 murine macrophage and HEK 293 human epithelial cell lines, pneumolysin-induced apoptosis is in part TLR4 dependent (34). Quantitative real-time PCR showed that primary neurons expressed virtually no TLR4 mRNA, whereas primary microglia (as a control) exhibited high levels of TLR4 mRNA (Fig. 6B). In accordance with this result, in situ hybridization revealed the presence of TLR4 in microglia but not in neurons (Fig. 6A). These findings indicate that apoptosis induction in primary rat neurons is not dependent on TLR4 expression.

DISCUSSION

We demonstrate that pneumolysin, one of the major pneumococcal exotoxins, induces the key cell death mechanisms of live pneumococci, i.e., disturbed calcium homeostasis, accumulation of ROS, mitochondrial damage, translocation of AIF into the cytosol, and execution of caspase-independent programmed cell death. Mitochondrial membranes represent an additional target within the cell. The ability of pneumolysin to induce AIF-mediated apoptosis coincides with its pore-forming activity. An interaction with TLR4 is not required in order to induce cell death. Moreover, the presence of pneumolysin inhibits the activation of caspase-3, possibly through upregulation of XIAP.

Mitochondrial damage has been described as a key event in neuronal cell death induced by live pneumococci (7). Pneumococci induce oxidative stress in neurons via their exotoxin H_2O_2, leading to the release of Ca^{2+} from intracellular stores such as the endoplasmic reticulum and influx from the extracellular space. The subsequent increase in cytoplasmic and mitochondrial Ca^{2+} levels is a key event in apoptosis models of diverse origins (29). It leads to depolarization and swelling of mitochondria, breakdown of the respiratory function, and the formation of transition pores in the mitochondrial membranes (14, 17). A vicious circle leads to further compromise of the

energy metabolism, production of ROS, and an ongoing increase in the Ca^{2+} level. Furthermore, leakage of toxic proteins such as cytochrome *c* and AIF from the mitochondria per se is able to initiate apoptosis (32). While according to this concept, mitochondrial compromise and apoptosis induction by pneumococci are regarded as secondary effects of a disturbed cytoplasmic homeostasis, our data support a novel role for pneumolysin as a direct inducer of mitochondrial dysfunction. The presence of the W433F mutation, which substantially (1,000-fold) decreases pore-forming activity, abolished the proapoptotic activities of pneumolysin and resulted in a preserved ultrastructure of the mitochondria and failure to release AIF. These findings suggest that damage of membrane integrity through pore formation is the basis of pneumolysin's mitochondrial toxicity. In our experiments, pneumolysin translocates to the mitochondria. Interestingly, the pore-forming toxin PorB of *Neisseria gonorrhoeae* has also been shown to transfer to mitochondria and induce apoptosis in Jurkat T cells (27). The exact mechanisms of mitochondrial targeting of PorB and pneumolysin are unknown.

Programmed cell death in pneumococcal disease features both classical caspase-dependent and caspase-independent types of apoptosis. In experimental pneumococcal meningitis in vivo, about half of the neuronal loss is caused by the contribution of bacterial factors, while the remaining half is the consequence of the host immune response (4, 19). Moreover, about half of the neuronal loss in vivo is prevented by broad-spectrum caspase inhibition (6), while in the absence of inflammation, neuronal apoptosis is caspase independent (7). Taking into account our present results, it can be concluded that in vivo, caspase activation is triggered by the host immune response, whereas live bacteria and pneumolysin induce AIF-dependent, caspase-independent apoptosis (4, 6, 7).

Addressing a possible impact of pneumolysin on host immunity, the toxin has indeed been shown to activate TLR4 and induce partially caspase driven apoptosis in nonneuronal cells (34). However, given the absence of TLR4 in primary rat neurons as well as the failure of pneumolysin to activate neuronal caspases, a major direct contribution of TLR4 signaling by pneumolysin to the induction of neuronal apoptosis is highly unlikely.

In vitro, live pneumococci induce rapid apoptosis of primary neurons. As a distinctive feature, activation of caspases does not occur; rather, neuronal apoptosis is mediated by the release of AIF from the mitochondria into the cytoplasm (2, 7). Large-scale DNA fragmentation has been reported as a typical feature of AIF-mediated apoptosis (13, 37). Our present data indicate that pneumolysin is the pneumococcal factor responsible for caspase-independent cell death induction. Pneumolysin has previously been shown to induce caspase-independent apoptosis in dendritic cells (11) and primary brain microvascular endothelial cells (2), and a proportion of caspase-independent pneumolysin toxicity was also observed in murine RAW 246.7 macrophages (ATCC) (34) and SH-SY5SY human neuroblastoma cells (36).

As an interesting principle of action, our findings suggest that pneumolysin itself is the factor by which *S. pneumoniae* influences the type of apoptosis in primary neurons. While the presence of pneumolysin in wild-type D39 pneumococci was associated with strictly caspase independent apoptosis, the pneumolysin-deficient Δ*plnA* mutant induced a marked and early activation of caspase-3. The shift to a caspase-independent type of apoptosis could be linked to the ability of pneumolysin to target mitochondrial membranes and release AIF as an inducer of caspase-independent apoptosis. However, the inhibition of staurosporine-induced caspase-3 activation and the upregulation of XIAP, a crucial endogenous regulator of cell survival (35), suggest an actively suppressive mechanism involving the inhibition of caspase activation.

In conclusion, pneumolysin is a major neurotoxin of *S. pneumoniae*. Characteristic features of apoptosis induced by live pneumococci, especially the absence of caspase activation, are mediated by pneumolysin. Targeting of mitochondria seems to be a central feature of pneumolysin's toxicity. Since the release of bioactive pneumolysin is potentiated by antibiotic-induced lysis of the bacterium, neutralizing this toxin is a potential strategy to reduce cell damage in invasive pneumococcal infections.

ACKNOWLEDGMENTS

This work was supported by grants from the Deutsche Forschungsgemeinschaft SFB 507/B6 (to J.S.B., O.H., and J.R.W.) and the Meningitis Research Foundation (to J.S.B. and J.R.W.).

We thank Renate Gusinda, Cordula Mahrhofer, and Gisela Duwe for excellent technical support.

REFERENCES

1. **Benton, K. A., M. P. Everson, and D. E. Briles.** 1995. A pneumolysin-negative mutant of *Streptococcus pneumoniae* causes chronic bacteremia rather than acute sepsis in mice. Infect. Immun. **63:**448–455.
2. **Bermpohl, D., A. Halle, D. Freyer, E. Dagand, J. S. Braun, I. Bechmann, N. W. Schroder, and J. R. Weber.** 2005. Bacterial programmed cell death of cerebral endothelial cells involves dual death pathways. J. Clin. Investig. **115:**1607–1615.
3. **Bhakdi, S., and J. Tranum-Jensen.** 1986. Membrane damage by pore-forming bacterial cytolysins. Microb. Pathog. **1:**5–14.
4. **Braun, J. S., J. E. Sublett, D. Freyer, T. J. Mitchell, J. L. Cleveland, E. I. Tuomanen, and J. R. Weber.** 2002. Pneumococcal pneumolysin and H_2O_2 mediate brain cell apoptosis during meningitis. J. Clin. Investig. **109:**19–27.
5. **Braun, J. S., R. Novak, G. Gao, P. J. Murray, and J. L. Shenep.** 1999. Pneumolysin, a protein toxin of *Streptococcus pneumoniae*, induces nitric oxide production from macrophages. Infect. Immun. **67:**3750–3756.
6. **Braun, J. S., R. Novak, K. H. Herzog, S. M. Bodner, J. L. Cleveland, and E. I. Tuomanen.** 1999. Neuroprotection by a caspase inhibitor in acute bacterial meningitis. Nat. Med. **5:**298–302.
7. **Braun, J. S., R. Novak, P. J. Murray, C. M. Eischen, S. A. Susin, G. Kroemer, A. Halle, J. R. Weber, E. I. Tuomanen, and J. L. Cleveland.** 2001. Apoptosis-inducing factor mediates microglial and neuronal apoptosis caused by pneumococcus. J. Infect. Dis. **184:**1300–1309.
8. **Breitschopf, H., G. Suchanek, R. M. Gould, D. R. Colman, and H. Lassmann.** 1992. In situ hybridization with digoxigenin-labeled probes: sensitive and reliable detection method applied to myelinating rat brain. Acta Neuropathol. **84:**581–587.
9. **Bronfman, M., G. Loyola, and C. S. Koenig.** 1998. Isolation of intact organelles by differential centrifugation of digitonin-treated hepatocytes using a table Eppendorf centrifuge. Anal. Biochem. **255:**252–256.
10. **Cockeran, R., A. J. Theron, H. C. Steel, N. M. Matlola, T. J. Mitchell, C. Feldman, and R. Anderson.** 2001. Proinflammatory interactions of pneumolysin with human neutrophils. J. Infect. Dis. **183:**604–611.
11. **Colino, J., and C. M. Snapper.** 2003. Two distinct mechanisms for induction of dendritic cell apoptosis in response to intact *Streptococcus pneumoniae*. J. Immunol. **171:**2354–2365.
12. **Comis, S. D., M. P. Osborne, J. Stephen, M. J. Tarlow, T. L. Hayward, T. J. Mitchell, P. W. Andrew, and G. J. Boulnois.** 1993. Cytotoxic effects on hair cells of guinea pig cochlea produced by pneumolysin, the thiol activated toxin of *Streptococcus pneumoniae*. Acta Otolaryngol. **113:**152–159.
13. **Cregan, S. P., A. Fortin, J. G. MacLaurin, S. M. Callaghan, F. Cecconi, S. W. Yu, T. M. Dawson, V. L. Dawson, D. S. Park, G. Kroemer, and R. S. Slack.** 2002. Apoptosis-inducing factor is involved in the regulation of caspase-independent neuronal cell death. J. Cell Biol. **158:**507–517.
14. **Crompton, M.** 1999. The mitochondrial permeability transition pore and its role in cell death. Biochem. J. **341:**233–249.
15. **Friedland, I. R., M. M. Paris, S. Hickey, S. Shelton, K. Olsen, J. C. Paton,**

and G. H. McCracken. 1995. The limited role of pneumolysin in the pathogenesis of pneumococcal meningitis. J. Infect. Dis. **172:**805–809.
16. **Gilbert, R. J., J. L. Jimenez, S. Chen, I. J. Tickle, J. Rossjohn, M. Parker, P. W. Andrew, and H. R. Saibil.** 1999. Two structural transitions in membrane pore formation by pneumolysin, the pore-forming toxin of *Streptococcus pneumoniae*. Cell **97:**647–655.
17. **Hajnoczky, G., E. Davies, and M. Madesh.** 2003. Calcium signaling and apoptosis. Biochem. Biophys. Res. Commun. **304:**445–454.
18. **Heiskanen, K. M., M. B. Bhat, H. W. Wang, J. Ma, and A. L. Nieminen.** 1999. Mitochondrial depolarization accompanies cytochrome *c* release during apoptosis in PC6 cells. J. Biol. Chem. **274:**5654–5658.
19. **Hoffmann, O., J. Zweigner, S. H. Smith, D. Freyer, C. Mahrhofer, E. Dagand, E. I. Tuomanen, and J. R. Weber.** 2006. Interplay of pneumococcal hydrogen peroxide and host-derived nitric oxide. Infect. Immun. **74:**5058–5066.
20. **Kooy, N. W., J. A. Royall, H. Ischiropoulos, and J. S. Beckman.** 1994. Peroxynitrite-mediated oxidation of dihydrorhodamine 123. Free Radic. Biol. Med. **16:**149–156.
21. **Lautenschlager, M., M. V. Onufriev, N. V. Gulyaeva, C. Harms, D. Freyer, U. Sehmsdorf, K. Ruscher, Y. V. Moiseeva, A. Arnswald, I. Victorov, U. Dirnagl, J. R. Weber, and H. Hörtnagl.** 2000. Role of nitric oxide in the ethylcholine aziridinium model of delayed apoptotic neurodegeneration in vivo and in vitro. Neuroscience **97:**383–393.
22. **Li, H., H. Zhu, C. J. Xu, and J. Yuan.** 1998. Cleavage of BID by caspase 8 mediates the mitochondrial damage in the Fas pathway of apoptosis. Cell **94:**491–501.
23. **Menzies, B. E., and I. Kourteva.** 1998. Internalization of *Staphylococcus aureus* by endothelial cells induces apoptosis. Infect. Immun. **66:**5994–5998.
24. **Mitchell, T. J., and P. W. Andrew.** 1997. Biological properties of pneumolysin. Microb. Drug Resist. **3:**19–26.
25. **Morgan, P. J., P. W. Andrew, and T. J. Mitchell.** 1996. Thiol-activated cytolysins. Rev. Med. Microbiol. **7:**221–229.
26. **Mosmann, T.** 1983. Rapid colorimetric assay for cellular growth and survival: application to proliferation and cytotoxicity assays. J. Immunol. Methods **65:**55–63.
27. **Müller, A., D. Günther, V. Brinkmann, R. Hurwitz, T. F. Meyer, and T. Rudel.** 2000. Targeting of the pro-apoptotic VDAC-like porin (PorB) of *Neisseria gonorrhoeae* to mitochondria of infected cells. EMBO J. **19:**5332–5343.
28. **Paton, J. C.** 1996. The contribution of pneumolysin to the pathogenicity of *Streptococcus pneumoniae*. Trends Microbiol. **4:**103–106.
29. **Rizzuto, R., P. Pinton, D. Ferrari, M. Chami, G. Szabadkai, P. J. Magalhaes, F. Di Virgilio, and T. Pozzan.** 2003. Calcium and apoptosis: facts and hypotheses. Oncogene **22:**8619–8627.
30. **Rubins, J. B., and E. N. Janoff.** 1998. Pneumolysin: a multifunctional pneumococcal virulence factor. J. Lab. Clin. Med. **131:**21–27.
31. **Rubins, J. B., D. Charboneau, J. C. Paton, T. J. Mitchell, P. W. Andrew, and E. N. Janoff.** 1995. Dual function of pneumolysin in the early pathogenesis of murine pneumococcal pneumonia. J. Clin. Investig. **95:**142–150.
32. **Saelens, X., N. Festjens, L. Vande Walle, M. van Gurp, G. van Loo, and P. Vandenabeele.** 2004. Toxic proteins released from mitochondria in cell death. Oncogene **23:**2861–2874.
33. **Schwartz, D. C., and C. R. Cantor.** 1984. Separation of yeast chromosome-sized DNAs by pulsed field gradient gel electrophoresis. Cell **37:**67–75.
34. **Srivastava, A., P. Henneke, A. Visintin, S. C. Morse, V. Martin, C. Watkins, J. C. Paton, M. R. Wessels, D. T. Golenbock, and R. Malley.** 2005. The apoptotic response to pneumolysin is Toll-like receptor 4 dependent and protects against pneumococcal disease. Infect. Immun. **73:**6479–6487.
35. **Stennicke, H. R., C. A. Ryan, and G. S. Salvesen.** 2002. Reprieval from execution: the molecular basis of caspase inhibition. Trends Biochem. Sci. **27:**94–101.
36. **Stringaris, A. K., J. Geisenhainer, F. Bergmann, C. Balshusemann, U. Lee, G. Zysk, T. J. Mitchell, B. U. Keller, U. Kuhnt, J. Gerber, A. Spreer, M. Bahr, U. Michel, and R. Nau.** 2002. Neurotoxicity of pneumolysin, a major pneumococcal virulence factor, involves calcium influx and depends on activation of p38 mitogen-activated protein kinase. Neurobiol. Dis. **11:**355–368.
37. **Susin, S. A., H. K. Lorenzo, N. Zamzami, I. Marzo, B. E. Snow, G. M. Brothers, J. Mangion, E. Jacotot, P. Costantini, M. Loeffler, N. Larochette, D. R. Goodlett, R. Aebersold, D. P. Siderovski, J. M. Penninger, and G. Kroemer.** 1999. Molecular characterization of mitochondrial apoptosis-inducing factor. Nature **397:**441–446.
38. **Susin, S. A., E. Daugas, L. Ravagnan, K. Samejima, N. Zamzami, M. Loeffler, P. Costantini, K. F. Ferri, T. Irinopoulou, M.-C. Prévost, G. Brothers, T. W. Mak, J. Penninger, W. C. Earnshaw, and G. Kroemer.** 2000. Two distinct pathways leading to nuclear apoptosis. J. Exp. Med. **192:**571–579.
39. **Tuomanen, E., H. Liu, B. Hengstler, O. Zak, and A. Tomasz.** 1985. The induction of meningeal inflammation by components of the pneumococcal cell wall. J. Infect. Dis. **151:**859–868.
40. **Winter, A. J., S. D. Comis, M. P. Osborne, M. J. Tarlow, J. Stephen, P. W. Andrew, J. Hill, and T. J. Mitchell.** 1997. A role for pneumolysin but not neuraminidase in the hearing loss and cochlear damage induced by experimental pneumococcal meningitis in guinea pigs. Infect. Immun. **65:**4411–4418.

Editor: J. N. Weiser